DOI: 10.1002/cbic.201100576

Mechanism-Oriented Redesign of an Isomaltulose Synthase to an Isomelezitose Synthase by Site-Directed Mutagenesis

Julian Görl, Malte Timm, and Jürgen Seibel*[a]

Dedicated to Professor Gerd Bringmann on the occasion of his 60th birthday.

An isomelezitose synthase was redesigned out of the sucrose isomerase from *Protaminobacter rubrum* for the synthesis of isomelezitose (6-O^F-glucosylsucrose), a potential nutraceutical. The variants F297A, F297P, R333K, F321A_F319A and E428D catalyze the formation of isomelezitose in up to 70% yield.

Introduction

The trisaccharide isomelezitose (6-O^F-glucosylsucrose, **1**, Scheme 1), recently found in honey,[1] has been identified as a potent nutraceutical candidate.[2]

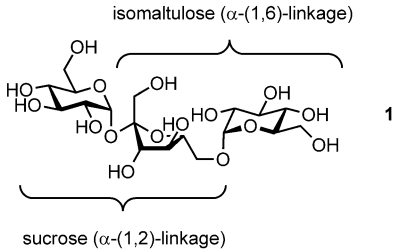

Scheme 1. The structure of the trisaccharide isomelezitose (**1**).

Isomelezitose is a substrate for bifidobacteria in the colon and thus has probiotic properties.[2] It is not cleaved either by salivary enzymes or bacteria of the pharynx or in the small intestine. Isomelezitose is noncariogenic, has a smaller calorific value in comparison to sucrose and is suitable for inclusion in foods for diabetics.[2] Due to the interest in this compound, an industrial process has been developed which uses immobilized cells of *Protaminobacter rubrum* (CBS 574.77) commonly used for the synthesis of isomaltulose from sucrose on an industrial scale (100 000 tons per annum),[3] forming **1** in 11% yield at 50 °C.[2] However, drawbacks of the process are high reaction temperature, which causes a decreased stability of the enzyme (at most 43 d compared to 200 d for isomaltulose production) and low yield, which results in the need for further concentration and purification steps.[2,3] As complete cells were used the enzyme forming the trisaccharide remained unknown.

Fujii et al. described a similar method and obtained the trisaccharide in 8% yield using immobilized cells from *S. plymuthica*.[4] Some α-glucosidases[4,5] of the family GH13 are responsible for the synthesis of **1** according to the carbohydrate-active enzymes (CAZy) database.[6] As an example, the formation of **1** as well as the synthesis of 4-O^F-glucosylsucrose and theanderose (6-O^G-glucosylsucrose) was observed by Inohara-Ochiai et al.[5] when incubating an α-glucosidase from *Bacillus sp.* SAM1606 with 60% (*w*/*v*) sucrose at 60 °C. Unfavorably, the enzyme preferentially catalyzes hydrolysis (71%).[7] Mutagenesis experiments performed by Inohara-Ochiai et al.[5,7] succeeded in changing the ratio of the obtained trisaccharides in favor of **1**, but the overall yield was reduced from 8 to 2%. Furthermore, hydrolysis was still the main reaction (90%).

Results and Discussion

Enzymes are highly efficient catalysts for stereoselective syntheses. However, the reactions are limited due to high substrate and product specificity. Our goal is to expand the synthetic repertoire of enzymes. Here we provide an example where an enzyme has been redesigned for efficient synthesis of isomelezitose (**1**). With the α-glucosidase from *B. sp.* SAM1606 which forms **1** as a starting point, the following steps were performed to obtain an isomelezitose synthase.

- Identification of glucansucrases which exhibit high sequence identity to the α-glucosidase from *B. sp.* SAM1606 utilizing alignment tools (BLAST,[8,9] ClustalW2[10]).
- Narrowing down the query to enzymes within the PDB which show high transfer activity and
- perform the desired α-(1,6)-glycosidic coupling reaction (mechanism-based analysis).
- Selection of promising amino acids for site-directed mutagenesis by sequence and structural alignments in combination with docking studies (estimation of space requirement and possible interactions for the catalytic process).

[a] *J. Görl, M. Timm, Prof. Dr. J. Seibel*
Institute of Organic Chemistry, Julius-Maximilians University Würzburg
Am Hubland, 97074 Würzburg (Germany)
E-mail: seibel@chemie.uni-wuerzburg.de

 © 2012 Wiley-VCH Verlag GmbH & Co. KGaA, Weinheim

- Site-directed mutagenesis to shift the product specificity to isomelezitose production.

Sequence and structure alignments and query refinements

Since the α-glucosidase from *B. sp.* SAM1606 synthesizes **1** as a side product[5] its sequence was applied in several alignments (BLAST,[8,9] ClustalW2[10]). The alignments revealed a large number of α-(1,6)-glucosidases from the GH13 family (α-amylase family, CAZy database[6]) to be most similar (>90% query coverage according to BLAST[8,9]).

For the generation of new enzyme specificities, directed evolution has been demonstrated to be a successful tool.[11–13] An alternative approach for some enzymes could involve site-directed mutagenesis.[14] For this, incorporating the knowledge of structure and function of a given enzyme involving detailed data on the reaction mechanism is a basic requirement for the selection of target sites for site-directed mutations.[15] Thus, only enzymes within the Protein Data Bank were further examined using 3D-Jury.[16] The α-glucosidase from *B. cereus* (80% sequence identity, 3D-Jury score 372.00) was predicted to have the highest similarity with the glucosidase from *B. sp.* SAM1606. Since the synthesis of **1** is a transfer reaction, we then focused on enzymes with a high transfer activity. The query revealed the sucrose isomerases (SIs, EC. 5.4.99.11, up to 99% transfer activity[17–20]) among which are SmuA from *P. rubrum* and MutB from *P. mesoacidophila* MX-45 (3D-Jury score: 365.00 and 361.33, respectively) to be most similar. The obtained sequences were aligned using ClustalW2[10] (Figure 1, visualization: Jalview[21]).

Next, we took a closer look on the product specificities and the reaction mechanism. The SIs catalyze the isomerisation of sucrose to isomaltulose (D-fructofuranosyl-(6,1)-α-D-glucopyranoside, **3**) and trehalulose (D-fructofuranosyl-(1,1)-α-D-glucopyranoside, **4**, Scheme 2). The formation of **1** was not yet observed and the structural determinants that enable the synthesis of **1** by α-glucosidases remain unknown. By site-directed mutagenesis we anticipated to generate a variant of the SI which performs the synthesis of **1**.

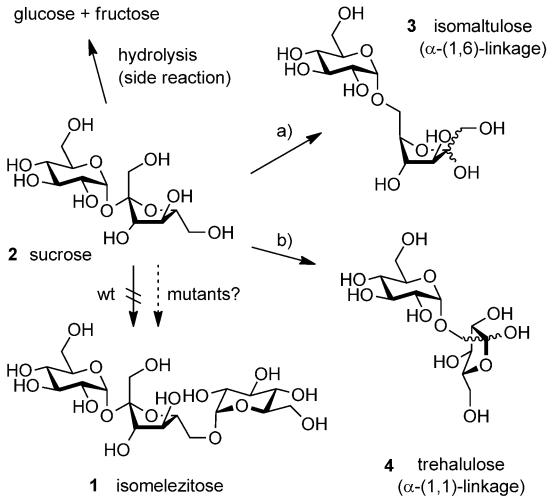

organism and gene	3	4	hydrolysis
a) isomaltulose synthase e.g. SmuA	75–85	5–9	5–10 %
Pall (*Klebsiella-enterobacter* sp. LX3)	60–80	5–20	0–10 %
b) trehalulose synthase e.g. MutB	8	91	1 %

Scheme 2. Product specificity of the different sucrose isomerases.[17–20]

Reaction mechanism, linkage and structure

Therefore, primary, secondary and tertiary structure of the SIs and related α-glucosidases were examined. Although the structures of the SIs are very similar (up to 80% sequence identity), the ratio of isomaltulose (**3**) to trehalulose (**4**) varies enormously depending on the originating organism (Scheme 2).[19,22–24] The isomaltulose synthase from *P. rubrum* (SmuA, 45% sequence identity to the α-glucosidase from *B. sp.* SAM1606, 95% transfer activity) catalyzes the desired α-(1,6)-coupling reaction, whereas the main product of MutB (trehalulose synthase from *P. mesoacidophila*) is trehalulose (**4**) (Scheme 2).[18]

Zhang et al. and Ravaud et al. recently published the structures of SmuA, MutB and Pall.[18,22,24] The enzymes consist of three domains: domain A containing the $(\beta/\alpha)_8$-barrel (TIM

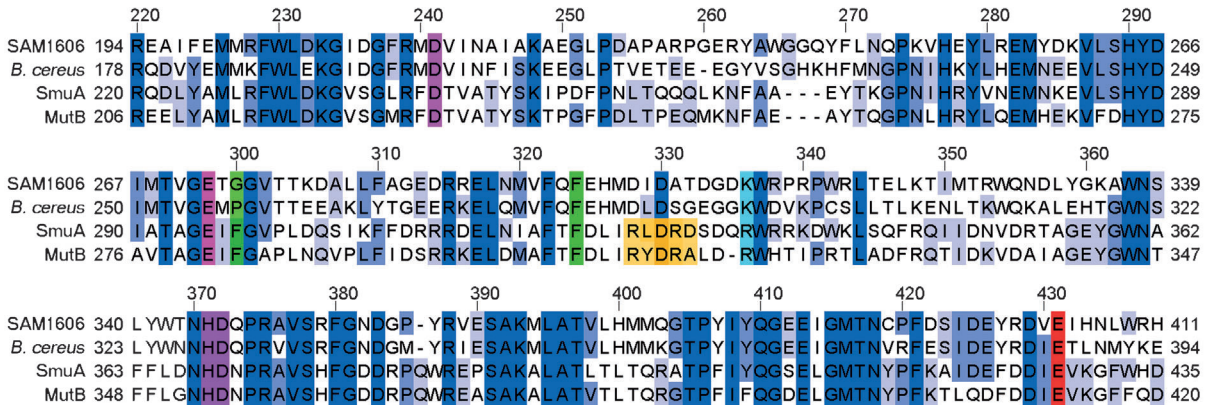

Figure 1. Part of the ClustalW2-Alignment of the α-glucosidase from *B. sp.* SAM1606 to enzymes within the PDB; blue: density represents identity, magenta: catalytic residues, orange: fructose binding site, green: entrance to active pocket; SmuA: SI from *P. rubrum*, MX-45: MutB, SI from *P. mesoacidophila* MX-45.

 © 2012 Wiley-VCH Verlag GmbH & Co. KGaA, Weinheim

barrel), a loop-rich N-terminal region (domain B) and domain C harboring several antiperiplanar β-sheets.

The residues D241, E295, H368 and D369 (magenta, SmuA numbering, Figure 1) were identified to catalyze the isomerization of **2** to **3**.[22,25,26] The reaction occurs by a so called "ping-pong" mechanism. D241 is the nucleophile which attacks the glycosidic bond and forms a covalent β-linked glucosyl–enzyme intermediate ("ping"). This is facilitated by E295 (acid/base catalyst) and D369 (transition-state stabilizer). Hence, the fructosyl residue is cleaved but remains inside the active site. The product specificity (ratio of **3**:**4**) is proposed to be determined by a unique fructosyl binding site (FBS, ^{325}RXDRX^{329}, +1 sub-site; orange, Figure 1) which is responsible for the correct orientation of the fructosyl moiety during the isomerization step (nucleophilic attack of the 6-OH of the fructosyl moiety on the ES-complex; "pong").[23] An aromatic clamp (F297, F321; green, Figure 1) at the entrance of the active pocket protects the ES-complex from attack by water.[18,24] In addition, only low yields (< 5.6%) were obtained in acceptor/substrate studies previously performed.[27] However, transfer reactions in higher yields are possible if the SI is mutated. Lee et al. demonstrated that isomaltose can be obtained in 19% yield by the SmuA variant R325K (part of FBS) with glucose as the acceptor.[25]

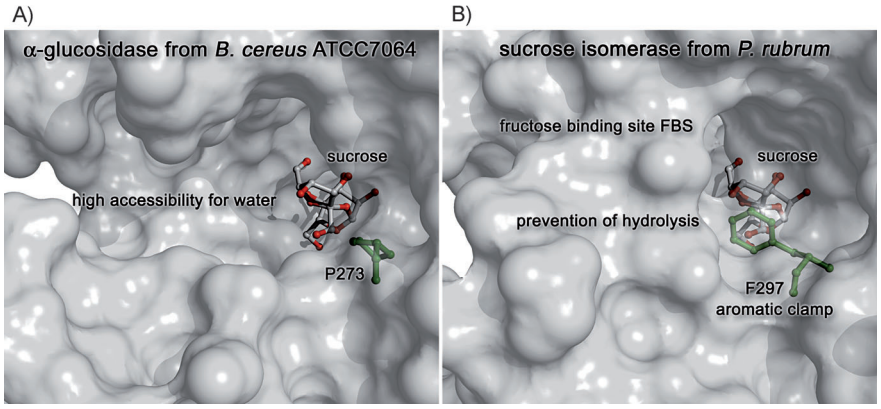

Figure 2. Comparison of the surface of the α-glucosidase from *B. cereus* (A) and the SI SmuA (B); the entrance is wide open in case of the α-glucosidase compared to the narrow entry of the SI preventing the hydrolysis (visualization: PyMOL 1.3).

Selection of amino acids for site-directed mutagenesis

With the knowledge of these previous studies, we aimed to redesign the isomaltulose synthase from *P. rubrum* into an isomelezitose synthase by site-directed mutagenesis. In addition to sequence alignments (Figure 1) it was helpful to compare the structure of SmuA with the α-glucosidase from *B. sp.* SAM1606. Due to the lack of a crystal structure of the α-glucosidase from *B. sp.* SAM1606, the α-glucosidase from *B. cereus* (80% sequence identity with SAM1606, 3D-Jury score 372.00) was used as a template for further alignments. The α-glucosidase from *B. cereus* (1UOK) was aligned to the SmuA (3GDB) using PyMol (Figure 2). The position of the substrate sucrose was estimated by an additional superposition of 2PWE (MutB, 80% identity to SmuA) to 3GDB/1UOK harboring a sucrose molecule in the active site (mutant E^{295}Q, SmuA-numbering).

Although the structures of both enzymes are similar, the α-glucosidase lacks the FBS of SmuA (Figure 2A). As a consequence, the α-glucosidase exhibits a wide-open entrance to the active pocket, favoring the hydrolysis but enabling synthesis of **1**. In contrast, the SmuA prevents hydrolysis due to its aromatic clamp, the FBS and a different loop/α-helix ^{257}QQQLKNFA^{265} (Nα5, Lee et al.[25]), but excludes trisaccharide formation (Figure 2B).

Docking studies

In order to estimate the space requirement of sucrose as an acceptor and to identify interactions between the enzyme and sucrose, docking studies were performed. For this, an enzyme–substrate (ES) complex was generated by superposition of the crystal structure from SmuA (3GDB) with MutB (2PWE) harboring a sucrose molecule in the active pocket due to the mutation E295Q. The fructosyl moiety was deleted (PyMOL) and the resulting structure was subsequently used as template in AutoDock 4.2.[28] In two calculations (100 runs each) fructose and sucrose respectively were applied as ligands in the docking process. We suggest that the results can help us to predict 1) whether sucrose fits into the narrow active pocket, 2) whether the fructosyl moiety of sucrose is able to adopt similar conformations as fructose alone and 3) which amino acids interact with sucrose as an acceptor.

Docking of fructose as ligand

Results differing by less than 1.0 Å root mean square deviation (rmsd) were clustered (top, Table 1). The numbering of the clusters depends on the highest binding energy of a conformation within a cluster.

Docking of sucrose as ligand

To simulate the formation of **1**, sucrose was used as a ligand in the docking-process. The docking results are listed in Table 1. This time, conformations with a clRMS value less than 1.5 Å were clustered since deviations were mostly caused by the orientation of the glucosyl moiety.

According to the docking results, sucrose fits in the active site of the glucopyranosyl–enzyme complex (Figure 3A). The fructosyl residue of sucrose (+1 sub-site, Figure 3A) is able to occupy similar conformations compared to fructose alone (not

 © 2012 Wiley-VCH Verlag GmbH & Co. KGaA, Weinheim

Table 1. The docking results are clustered und sorted by binding energy.

Docking (rmds)	Cluster[a]	Number of conformations	Highest binding energy [kcal mol^{-1}][b]
	1	64	−4.77
ES-complex + fructose	2–3	3	−4.57
(1.0 Å)	4	13	−4.09
	5–13	20	−3.94
	1	57	−6.52
ES-complex + sucrose	2	13	−4.77
(1.5 Å)	3	6	−1.79
	4–15	24	−1.90
	1	17	−7.06
ES-complex F297A +	2–3	12	−7.01
sucrose (1.5 Å)	4	6	−6.82
	5–43	65	−6.76

[a] The numbering of the clusters depends on the highest binding energy of a conformation within a cluster; [b] The binding energy was calculated by AutoDock 4.2.

shown) with C-6′ in position for the nucleophilic attack of the glucopyranosyl–enzyme complex.

Selection of targets for site-directed mutagenesis

On one hand, for the synthesis of **1**, binding of sucrose as an acceptor must be favored compared to fructose. On the other, we aimed to prevent hydrolysis. The isomerization of sucrose to isomaltulose is a highly efficient reaction. We think that the formation of the β-glucopyranosyl–enzyme complex followed by the nucleophilic attack of the 6′-OH group of fructose is concerted. This would explain why no hydrolysis takes place. We conclude that the FBS is necessary for this concerted process. Previous mutations of the FBS led to more hydrolysis, supporting our suggestions.[25] Thus, the FBS itself should not be mutated. Furthermore, we presumed that the bulky glucosyl moiety of sucrose as an acceptor might prohibit reactive conformations of the fructosyl moiety. Therefore, we aimed to enlarge the +2 subsite (Figure 3 A) while retaining the polarity of the +2 subsite.

With respect to the previous alignments, Phe297 (green, Figures 1, 3; Table 2) was mutated to Ala and Pro to enlarge the entrance of the active pocket. Our docking studies reveal that rotamers (not shown) of Arg333 (cyan, Figures 1, 3; +2 subsite; Table 2), which was supposed to provide H-bonds to the fructosyl moiety,[18] are able to interact with the fructosyl (1′-OH, ca. 2.5 Å) and the 6-OH group of the glucosyl residue of sucrose (ca. 2.7 Å) during the transfer reaction. In addition, whereas Arg333 is conserved in the SIs it is substituted by Lys in case of the α-glucosidase from *B. sp.* SAM1606. Thus, we mutated Arg333 to Lys. In addition, Glu428 (red, Figures 1, 3; Table 2) was substituted by Asp since it may interact with su-

Table 2. Performed mutations, their location within the protein and observed isomelezitose production (enzyme conc. 0.1 g L^{-1}, Sorensen buffer (50 mM, pH 7.0, 30 °C).

Mutation	Location/ proximity	Isomelezitose synthesis	Remaining transfer activity
F297A	aromatic clamp	yes	4%[a]
F297P	aromatic clamp	yes	< 1%[a]
F321A	aromatic clamp	hydrolysis	–
R333K	+2 subsite, opposite of F297 and F321	yes	13%[a]
E428D	opposite to FBS, +1 subsite	yes	[b]
R456K	in between −1 and +1 subsite	no	inactive[c]
F321A_F319A	aromatic clamp	yes	[b]
F297A_R333K	aromatic clamp, +2 subsite	yes	[b]

[a] No Michaelis–Menten kinetic; only valid at a concentration of 200 mM sucrose, 100% corresponds to the activity of isomaltulose formation by the wild-type enzyme. [b] Not determined due to low activity, but formation is observed on TLC. [c] No activity detected.

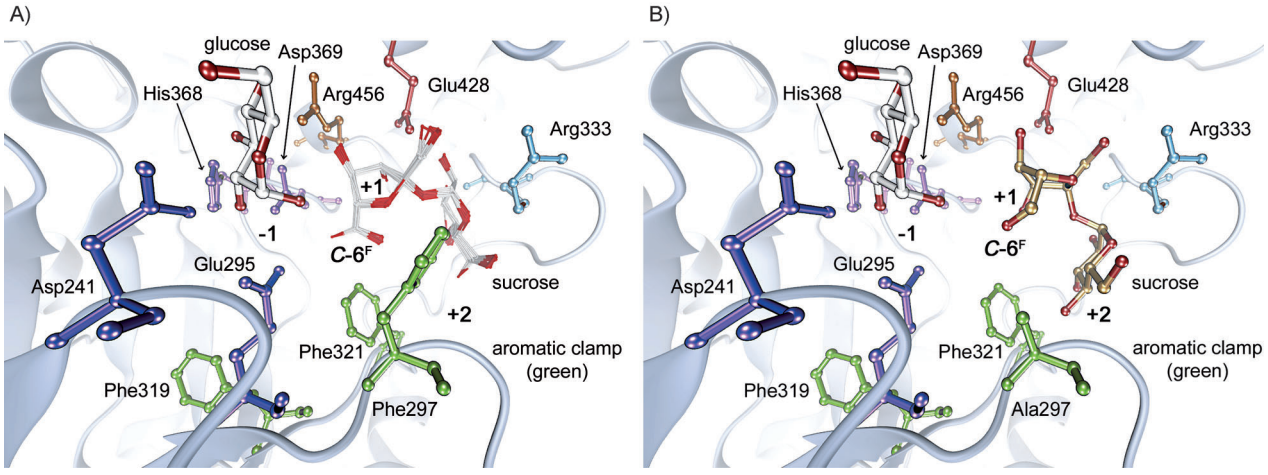

Figure 3. A) Docking of sucrose to the generated enzyme–substrate complex (visualization: VMD 1.9[29,30]). B) Within cluster 4 the fructosyl residue of sucrose is able to obtain new, more flexible conformations compared to the wild-type enzyme.

 © 2012 Wiley-VCH Verlag GmbH & Co. KGaA, Weinheim

crose (possible H-bond with 2′-OH and 3′-OH of fructose, +1 sub-site) as well as Arg456 (orange, Figures 1, 3; Table 2) which is positioned between the +1 and −1 subsites.

The desired variants were created in silico (PyMOL Mutagenesis Tool) and similar AutoDock studies were carried out. As an example, Figure 3B shows the docking of sucrose to the simulated ES-complex of variant F297A. Cluster 1 matches the conformation of the sucrose in the previous docking experiments, whereas cluster 4 adopts new conformations for the fructosyl residue. These conformations are probably caused by a different positioning of the glucosyl moiety. Its calculated binding energy (−6.82 kcal mol^{-1}, Table 1) is higher than the binding energy of cluster 1 (−7.06 kcal mol^{-1}, Table 1), but still exceeds the highest binding energy of the wild-type enzyme (−6.52 kcal mol^{-1}, Table 1). Besides the influence of the mutation on the fructose binding and hydrolysis, this could reflect an increased possibility for the fructosyl residue to occupy reactive conformations for isomelezitose synthesis.

Site-directed mutagenesis, determination of product specificity and kinetic data

By site-directed mutagenesis we successfully generated multiple variants, which are able to synthesize **1** and have minor hydrolysis activity (<5%, determined using TLC). All performed mutations are listed in Table 2. In particular, F297A and R333K still preserved 4 and 13% activity (calculated by the method of Vilozny et al.,[31] Table 3) compared to isomaltulose formation by the wild-type enzyme. The mutations F297P and E428D as well as the combinations F297A_R333K and F321A_F319A lead to a significant decrease in activity (Tables 2, 3). For these variants the formation of the trisaccharide was observed using TLC and **1** was isolated in similar yields (for example, 70% for the variant F321A_F319A), but we were unable to measure reliable kinetic data. R456K showed nearly no activity, whereas only hydrolysis was observed for F321A (Tables 2, 3).

Interestingly, the Michaelis–Menten plots of the variants show linear regressions instead of hyperbolic slopes. Even with 1.2 M sucrose no saturation of initial velocity (v_i) was observed. This kind of progression has been previously observed[33] and can either be explained by allosteric effects or a switch in the reaction mechanism. Since two molecules of sucrose are needed for synthesis of **1**, the kinetic reaction order can differ strongly from the facilitated Michaelis–Menten plot.[33] For this reason, K_M could not be calculated and the kinetic parameters given in Tables 2 and 3 are only valid for the described conditions (200 mM sucrose).

Similarly with some variants of the α-glucosidase from *B. sp.* SAM1606, the formation of **1** was fast at the beginning with no detectable production of **3**, **4** or monosaccharides (hydrolysis). **1** can be obtained on a preparative scale in 70% yield based on sucrose consumed (200 mM sucrose, 50 mM Sorensen buffer pH 6.0, 25 °C, 17 h). After long time the reaction proceeds with the formation of **3**. To optimize the process, **1** has to be continuously isolated.

The structure of **1** was confirmed by NMR. The linkages of the three glycosyl moieties were determined by two-dimensional correlation spectroscopies (HSQC, HMBC, TOCSY, NOESY). The correlation signal between H-1 (5.42 ppm, d, 1H) of glucose and C-2′ (104.1 ppm) of fructose (Figure 4, top) and the ^3J coupling constant of H-1 (3.90 Hz) show the α-(1,2)-linkage between fructose and glucose (=sucrose). In addition, the correlation signal between H-1″ (4.96 ppm, d, 1H; ^3J= 3.73 Hz) and C-6′ of fructose verifies the α-(1,6)-linkage (Figure 4, top). Furthermore, the correlation signals between the diastereotopic protons H-6′ and C-1″ are observed

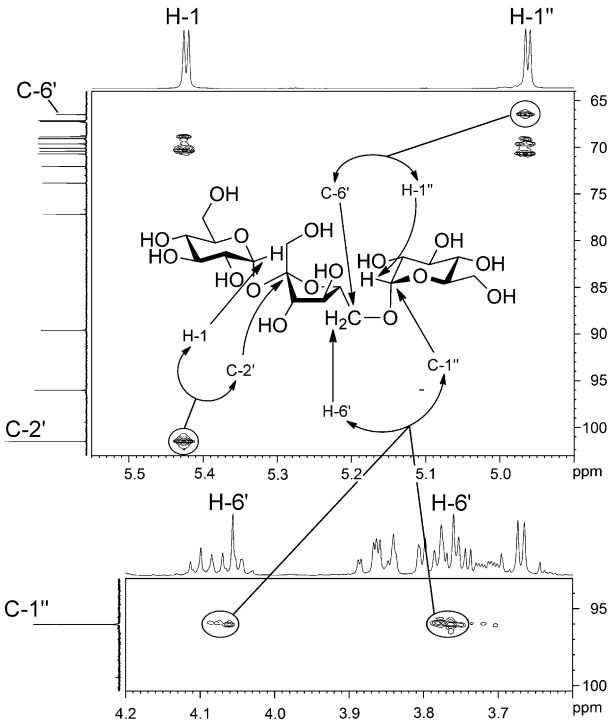

Figure 4. Close-up views on the HMBC spectrum of isomelezitose.

Table 3. Kinetic data of the wild-type and the variants (0.1 g L^{-1}) in Sorensen buffer (50 mM, pH 7.0), 30 °C.

Variant	V_{max} [mM s^{-1} 10^{-3}]	K_M [mM]	k_{cat} [s^{-1}]	k_{cat}/K_M [mM^{-1} s^{-1}]	Specific activity [U mg^{-1}]
wt (pH 5.5, 25 °C)[32]	–	32	42.1×10^3	1301.0	500
wt (pH 7.0, 30 °C)	35.8±0.4	22±1	30±5	1.4±0.2	1.1±0.1
F297A[a]	1.54±0.08	–	1.3±0.2	–	0.046±0.005
F297P[a]	0.24±0.02	–	0.20±0.03	–	$7.2\times10^{-3}\pm0.9\times10^{-3}$
R333K[a]	4.6±0.6	–	3.8±0.6	–	0.14±0.02
F321A_F319A	[b]	[b]	[b]	[b]	[b]
F297A_R333K	[b]	[b]	[b]	[b]	[b]
E428D	[b]	[b]	[b]	[b]	[b]

[a] No Michaelis–Menten kinetics; only valid at a concentration of 200 mM sucrose; [b] Not determined due to low activity but formation is observed on TLC.

 © 2012 Wiley-VCH Verlag GmbH & Co. KGaA, Weinheim

(Figure 4, bottom). All other signals are in agreement with the structure.

Conclusion

The redesign of enzymes for new substrates and/or functions is a key endeavor of biocatalysis and the enzymatic synthesis of carbohydrates has been proven to be nontrivial in this regard. We succeeded with one single amino acid exchange, R333K, to yield up to 70% isomelezitose (**1**), keeping in mind that no activity was observed with the wild-type enzyme. In conclusion, the scope of an enzyme was enhanced by site-directed mutagenesis. Sequence and structure alignments as well as mechanism-based computational docking studies were utilized to create an isomelezitose synthase out of the sucrose isomerase from *Protaminobacter rubrum*. An industrial process by using this enzyme as an immobilized catalyst could be envisaged.

Experimental Section

AutoDock studies: The docking experiments were carried out with AutoDockTools 1.5.4[28] with AutoDock version 4.2. An enzyme–substrate complex was generated by superposition of the crystal structure from SmuA (3GDB) with MutB (2PWE) harboring sucrose in the active pocket due to the mutation E295Q. The fructosyl moiety was deleted (PyMOL, version 1.3, Schrödinger, LLC,[34]) and the resulting complex was applied in AutoDock as a macromolecule file. Mutated amino acids (introduced with the PyMOL mutagenesis tool) were set to flexible as their conformation may vary. The conformations of sucrose and fructose (ligand) were adopted from the crystal structure 1GI (amylosucrase from *Neisseria polysaccharea*, 2.0 Å resolution) harboring sucrose in the active site. In the case of fructose, the glucosyl moiety was deleted from sucrose (PyMOL). 100 runs were performed for each docking experiment. The results were clustered by root mean square deviation (rmsd, 1.0 Å for fructose and 1.5 Å for sucrose as ligand) and ranked by binding energy calculated with AutoDock 4.2.

Oligonucleotides: Oligonucleotides were obtained from biomers.net (Ulm, Germany). Primers (Table 4) for subcloning of the sucrose isomerase from *Protaminobacter rubrum* CBS 547.77 (GenBank accession number CQ765969): for_SalI 5′-TAT AGT CGA CCC CGT CAA GGA TTG AAA ACT GC-3′ and rev_NotI 5′-ATA TGC GGC CGC TTA TTG ATT TAG TTT ATA AAC CCC-3′. PCRs were performed with a PCR MasterCycler personal instrument (Eppendorf).

Bacterial strains, plasmids and culture conditions: *Escherichia coli* TOP10 and *Escherichia coli* BL21 Star (both Invitrogen) were used for cloning procedures and protein expression, respectively. *Protaminobacter rubrum* CBS 547.77 was obtained from the Centraalbureau voor Schimmelcultures (Utrecht, Netherlands). The amplified gene was digested with SalI and NotI (both Fermentas) and subcloned into a pET-32a vector (Merck). The bacteria, harboring the recombinant plasmid (wild-type or mutant) were routinely grown at 37 °C in lysogeny broth medium (250 mL), supplemented with ampicillin (200 mg L^{-1}, LB-Amp).

General techniques: PCRs, agarose gel electrophoresis and transformations were carried out according to standard protocols.[35]

Site-directed mutagenesis of the SI: Mutations were introduced using the QuikChange II Site-Directed Mutagenesis Kit (Agilent Technologies Inc., Santa Clara, USA) following the manufacturer's manual. The digested (DpnI) PCR products were transformed into electro-competent cells of *E. coli* TOP10 and the transformants were selected with LB-Amp. The plasmids were isolated using the E.Z.N.A. Plasmid Mini Kit I (OMEGA Bio-Tek, Norcross, USA). The desired mutations were confirmed by DNA sequencing (GATC biotech AG, Konstanz, Germany).

Table 4. Primers for the desired mutations; mutated bases are underlined.

Mutation	Primer
R333K	For 5′-CGA GAC TCT GAT CAA AAG TGG CGT CGA AAA GAT TGG-3′ Rev 5′-CCA ATC TTT TCG ACG CCA CTT TTG ATC AGA GTC TCG-3′
F297A	For 5′-CC GGT GAA ATC GCT GGC GTA CCC-3′ Rev 5′-GGG TAC GCC AGC GAT TTC ACC GG-3′
F297P	For 5′-CC GGT GAA ATC CCT GGC GTA CCC-3′ Rev 5′-GGG TAC GCC AGG GAT TTC ACC GG-3′
F319A_ F321A	For 5′-CTG AAC ATT GCA GCT ACC GCT GAC TTA ATC AGA CTC G-3′ Rev 5′-C GAG TCT GAT TAA GTC AGC GGT AGC TGC AAT GTT CAG-3′
F321A	For 5′-CTG AAC ATT GCA TTT ACC GCT GAC TTA ATC AGA CTC G-3′ Rev 5′-C GAG TCT GAT TAA GTC AGC GGT AAA TGC AAT GTT CAG-3′
E428D	For 5′-C GAT GAT ATT GAC GTG AAA GGT TTT TGG C-3′ Rev 5′-G CCA AAA ACC TTT CAC GTC AAT ATC ATC G-3′
R456K	For 5′-CGC CTG ACG AGC AAG GAT AAC AGC C-3′ Rev 5′-G GCT GTT ATC CTT GCT CGT CAG GCG-3′

Enzyme production by fermentation: Precultures were grown in test tubes containing LB-Amp (5 mL) at 37 °C with shaking at 250 rpm for 17 h. The precultures were transferred into LB-Amp (250 mL) and incubated at 37 °C with shaking at 160 rpm. The cultures were induced with isopropyl-β-D-thiogalactopyranoside (IPTG) at an OD_{600} value of approximately 0.6 to a final concentration of 0.50 mM and incubated for 17 h at 20 °C with shaking at 160 rpm. The cells were collected by centrifugation at 6400 *g* and 4 °C, washed with Sorensen buffer (10 mL, 50 mM, pH 8.0), resuspended in the same buffer (6.25 mL) supplemented with β-mercaptoethanol (5 mM) and imidazole (10 mM). The cells were disrupted by sonification (4 min pulsed operation at 50 W).

Enzyme purification: The pET-32a vector introduced an N-terminal His_6 tag into the expressed proteins. After sonification, cells were sedimented (10 min, 13300 *g*, 4 °C), and the proteins were isolated from the supernatants using HIS-Select Nickel Affinity Gel (Sigma–Aldrich) following the manufacturer's manual. The eluted proteins were rebuffered in 50 mM Sorensen buffer (pH 7.0) utilizing HiTrap desalting columns (Amersham Biosciences Europe GmbH, Freiburg, Germany) according to the manufacturer's manual. The proteins were concentrated with Vivaspin 500 (10000 MWCO PES) concentrators (Sartorius Stedim Biotech GmbH). Protein concentration was determined by the Bradford assay with bovine serum albumin as standard. Purification was checked by SDS-PAGE using pre-cast gels (VarioGel, Anamed Elektrophorese, Groß-Bieberau, Germany) with PageRuler unstained protein Ladder (Fermentas) as standard.

Enzyme assays: Enzyme reactions were carried out in Sorensen buffer (50 mM, pH 6.6) containing the purified protein (0.1 g L^{-1}) and sucrose (100 mg mL^{-1}) in a total volume of 20 μL. The reaction mixture was incubated at 30 °C with shaking at 750 rpm. Samples

 © 2012 Wiley-VCH Verlag GmbH & Co. KGaA, Weinheim

(1 μL) were collected, diluted with H_2O (99 μL, final sugar concentration of 1 mg mL^{-1}) and stored at −20 °C.

Enzyme kinetics: Kinetic data were collected utilizing an enzyme assay developed by *Vilozny* et al. 2009.[31] The boronic acid *N*,*N*′-bis-(benzyl-4-boronic acid)-4,4′-bipyridinium dibromide (4,4′-*m*-BBV), which was synthesized as described elsewhere,[36] was used as a quencher and 8-hydroxypyrene-1,3,6-trisulfonic acid trisodium salt (HPTS, Sigma–Aldrich) as a fluorescent dye. 20 μL reactions containing 4,4′-*m*-BBV (2.05 mM), HPTS (16.7 μM) and enzyme (0.1 g L^{-1}) in Sorensen buffer (50 mM, pH 7.0) were performed in 384-well plates. For the Michaelis–Menten plot the initial concentration of sucrose was varied from 0.0625–600 g L^{-1}. The change of fluorescence F_t (t = time, λ_{ex} = 360 nm, λ_{em} = 535 nm) was continuously monitored (interval of 30 s for 15 min) in a GENios well-plate reader (TECAN Austria GmbH) at 30 °C. Assays without enzyme were used as blank. The blank-corrected ratio F_t/F_0 was converted into concentrations by using a linear calibration of fructose/isomaltulose at different concentrations. The initial velocity (v_i) was obtained by linear regression of the concentration of the detected sugar over time. The plots of the variants showed no hyperbolic slope, instead linear regressions (R > 99%) were obtained. No saturation was observed even at 1.2 M sucrose. For this reason, K_M could not be calculated and the kinetic parameters are only valid at 200 mM sucrose [enzyme (0.1 g L^{-1}) in Sorensen buffer (50 mM, pH 7.0)].

Thin-layer chromatography: To monitor the progress of product formation diluted samples (1:100 with water) of the enzyme assays were applied onto silica thin-layer chromatography plates (20 cm x 20 cm TLC aluminum sheets, silica gel 60 F254 with concentrating zone with dimensions of 20 cm × 2.5 cm; Merck). Standard solutions were prepared containing the monosaccharides D-glucose, sucrose, isomaltulose and isomelezitose in different concentrations (0.0625 g L^{-1}-1.00 g L^{-1}). The carbohydrates were separated using two ascents (90 min) with water/2-propanol/ethyl acetate (1:3:6 *v*/*v*/*v*) as solvent system. Spots were detected by dipping the plates into the detecting reagent 0.3% *N*-(1-naphthyl)ethylenediamine (Fluka) with 5% concentrated sulfuric acid in methanol and heating in an oven (120 °C, 5 min). The consumption of sucrose and the yields of the products (isomelezitose and isomaltulose) were calculated by densitometric measurement of the spots (Bio-Imaging system, biostep GmbH, Jahnsdorf, Germany) using greyscale calibration with fructose, glucose, sucrose, isomaltulose and isomelezitose as standards.

Isolation and characterization of isomelezitose (β-D-fructofuranosyl-(2,1)-α-D-glucopyranosyl-(6,1)-α-D-glucopyranoside): The enzyme activity assay was performed in Sorensen buffer (50 mM, pH 7.0) with enzyme (0.1 g L^{-1}), sucrose (526 μmol, final concentration: 100 g L^{-1}), total volume 1.8 mL. After incubation for 17 h (25 °C with shaking at 750 rpm), the enzyme was inactivated by heating to 95 °C for 5 min. The resulting precipitate was separated by centrifugation and the supernatant was evaporated under reduced pressure. The residual carbohydrates were isolated by column chromatography (silica gel 0.04–0.063 mm, Macherey–Nagel) using the same solvent system water/2-propanol/ethyl acetate (1:3:6 *v*/*v*/*v*). The fractions containing the desired carbohydrate were pooled and the solvent was evaporated under reduced pressure yielding 30.0 mg (59.4 μmol, 70% based on the amount of sucrose consumed (58 mg, 169 μmol), variant: F321A_F319A) of the trisaccharide. ^{1}H NMR (600 MHz) and ^{13}C NMR (150 MHz,) were recorded on Bruker AMX 600 instruments using D_2O (δ = 4.79) as the solvent and the internal ^{1}H and acetic acid (21.03 ppm) as ^{13}C standard. MALDI-TOF mass spectra were obtained on a Bruker Daltonics-Microflex MALDI-TOF instrument with 2,5-dihydroxybenzoic acid (DHB) as matrix. ^{1}H NMR (600 MHz, D_2O, acetic acid, 25 °C): δ = 5.42 (d, J = 3.90 Hz, 1H; H-1), 4.96 (d, J = 3.73 Hz, 1H; H-1″), 4.21 (d, J = 8.60 Hz, 1H; H-3′), 4.10 (t, J = 8.60 Hz, 1H; H-4′), 4.06–4.03 (m, 2H; H-5′, H-6′), 3.86 (dd, J = 12.3, 2.30 Hz, 1H; H-6a), 3.86 (m, 2H; H-6″a, H-5), 3.81–3.74 (m, 5H; H-6b, H-3, H-6″b, H-3″, H-6′), 3.72 (ddd, J = 10.0, 4.67, 2.30 Hz, 1H; H-5″), 3.67 (d, J = 5.28, 2H; H-1′), 3.57–3.54 (m, 2H; H-2, H-2″), 3.46–3.43 (m, 2H; H-4, H-4″); ^{13}C NMR (150 MHz, D_2O, acetic acid, 25 °C): 101.5 (C-2′), 96.02 (C-1″), 89.61 (C-1), 77.17 (C-5′), 73.84 (C-3′), 72.05 (C-4′), 70.70 (C-3″), 70.42 (C-3), 70.10 (C-5), 69.64 (C-5″), 69.07 (C-2″), 68.87 (C-2), 67.21, 67.14 (C-4, C-4′), 66.48 (C-6′), 59.28 (C-1′), 58.23 (C-6″), 58.05 (C-6); MS: *m*/*z*: 527 [*M*+Na]$^+$.

Acknowledgements

This work was supported by the DFG (SFB578).

Keywords: biocatalysis · enzyme engineering · isomelezitose · oligosaccharides · sucrose isomerase

[1] J. Gómez Bárez, R. Garcia-Villanova, S. Elvira Garcia, A. González Paramás, *Chromatographia* **1999**, *50*, 461–469.
[2] V. M. Munir, *Vol. WO9922013* (Ed.: M. M. Suedzucker AG, Mannheim/Ochsenfurt, M. Vogel), Europe, **1999**.
[3] K. Buchholz, J. Seibel, *Carbohydr. Res.* **2008**, *343*, 1966–1979.
[4] S. Fujii, S. Kishihara, M. Komoto, J. Shimizu, *J. Sci. Food Agric.* **2000**, *30*, 339–344.
[5] M. Inohara-Ochiai, M. Okada, T. Nakayama, H. Hemmi, T. Ueda, T. Iwashita, Y. Kan, Y. Shibano, T. Ashikari, T. Nishino, *J. Biosci. Bioeng.* **2000**, *89*, 431–437.
[6] B. Henrissat, G. Davies, *Curr. Opin. Struct. Biol.* **1997**, *7*, 637–644.
[7] M. Okada, T. Nakayama, A. Noguchi, M. Yano, H. Hemmi, T. Nishino, T. Ueda, *J. Mol. Catal. B* **2002**, *16*, 265–274.
[8] S. F. Altschul, T. L. Madden, A. A. Schaffer, J. Zhang, Z. Zhang, W. Miller, D. J. Lipman, *Nucleic Acids Res.* **1997**, *25*, 3389–3402.
[9] S. F. Altschul, J. C. Wootton, E. M. Gertz, R. Agarwala, A. Morgulis, A. A. Schaffer, Y. K. Yu, *FEBS J.* **2005**, *272*, 5101–5109.
[10] R. Chenna, H. Sugawara, T. Koike, R. Lopez, T. J. Gibson, D. G. Higgins, J. D. Thompson, *Nucleic Acids Res.* **2003**, *31*, 3497–3500.
[11] K. E. Jaeger, T. Eggert, A. Eipper, M. T. Reetz, *Appl. Microbiol. Biotechnol.* **2001**, *55*, 519–530.
[12] M. T. Reetz, *Angew. Chem.* **2001**, *113*, 292–320; *Angew. Chem. Int. Ed.* **2001**, *40*, 284–310.
[13] F. H. Arnold, *Acc. Chem. Res.* **1998**, *31*, 125–131.
[14] C. P. Strube, A. Homann, M. Gamer, D. Jahn, J. Seibel, D. W. Heinz, *J. Biol. Chem.* **2011**, *286*, 17593–17600.
[15] M. Lehmann, L. Pasamontes, S. F. Lassen, M. Wyss, *Biochim. Biophys. Acta Protein Struct. Mol. Enzymol.* **2000**, *1543*, 408–415.
[16] K. Ginalski, A. Elofsson, D. Fischer, L. Rychlewski, *Bioinformatics* **2003**, *19*, 1015–1018.
[17] Y. Nagai, T. Sugitani, K. Tsuyuki, *Biosci. Biotechnol. Biochem.* **1994**, *58*, 1789–1793.
[18] S. Ravaud, X. Robert, H. Watzlawick, R. Haser, R. Mattes, N. Aghajari, *FEBS Lett.* **2009**, *583*, 1964–1968.
[19] L. Wu, R. G. Birch, *Appl. Environ. Microbiol.* **2005**, *71*, 1581–1590.
[20] D. Zhang, X. Li, L. H. Zhang, *Appl. Environ. Microbiol.* **2002**, *68*, 2676–2682.
[21] A. M. Waterhouse, J. B. Procter, D. M. A. Martin, M. Clamp, G. J. Barton, *Bioinformatics* **2009**, *25*, 1189–1191.
[22] D. Zhang, N. Li, S. M. Lok, L. H. Zhang, K. Swaminathan, *J. Biol. Chem.* **2003**, *278*, 35428–35434.
[23] D. Zhang, N. Li, K. Swaminathan, L. H. Zhang, *FEBS Lett.* **2003**, *534*, 151–155.
[24] S. Ravaud, X. Robert, H. Watzlawick, R. Haser, R. Mattes, N. Aghajari, *J. Biol. Chem.* **2007**, *282*, 28126–28136.

 © 2012 Wiley-VCH Verlag GmbH & Co. KGaA, Weinheim

[25] H. C. Lee, J. H. Kim, S. Y. Kim, J. K. Lee, *Appl. Environ. Microbiol.* **2008**, *74*, 5183 – 5194.
[26] A. Aroonnual, T. Nihira, T. Seki, W. Panbangred, *Enzyme Microb. Technol.* **2007**, *40*, 1221 – 1227.
[27] T. Veronese, P. Perlot, *FEBS Lett.* **1998**, *441*, 348 – 352.
[28] M. F. Sanner, *J. Mol. Graphics* **1999**, *17*, 57 – 61.
[29] W. Humphrey, A. Dalke, K. Schulten, *J. Mol. Graph.* **1996**, *14*, 33 – 38.
[30] J. E. Stone, *Masters Thesis*, University of Missouri – Rolla (USA), **1998**.
[31] B. Vilozny, A. Schiller, R. A. Wessling, B. Singaram, *Anal. Chim. Acta* **2009**, *649*, 246 – 251.
[32] S. Ravaud, H. Watzlawick, R. Haser, R. Mattes, N. Aghajari, *Acta Crystallogr. Sect. F Struct. Biol. Cryst. Commun.* **2006**, *62*, 74 – 76.
[33] E. J. Hehre, C. F. Brewer, D. S. Genghof, *J. Biol. Chem.* **1979**, *254*, 5942 – 5950.
[34] *The PyMOL Molecular Graphics System*, Version 1.3, Schrodinger, LLC, **2010**.
[35] J. Sambrook, D. W. Russell, *Molecular Cloning: A Laboratory Manual, Vols. 1 – 3*, 3rd ed., Cold Spring Harbor Laboratory Press, New York, **2001**.
[36] D. B. Cordes, S. Gamsey, Z. Sharrett, A. Miller, P. Thoniyot, R. A. Wessling, B. Singaram, *Langmuir* **2005**, *21*, 6540 – 6547.

Received: September 7, 2011
Published online on November 29, 2011

 © 2012 Wiley-VCH Verlag GmbH & Co. KGaA, Weinheim